

Particle in a box with a time-dependent δ -function potential

Seung Ki Baek,^{1,*} Su Do Yi,² and Minjae Kim¹

¹*Department of Physics, Pukyong National University, Busan 48513, Korea*

²*Department of Physics and Astronomy,
Seoul National University, Seoul 08826, Korea*

Abstract

In quantum information processing, one often considers inserting a barrier into a box containing a particle to generate one bit of Shannon entropy. We formulate this problem as a one-dimensional Schrödinger equation with a time-dependent δ -function potential. It is a natural generalization of the particle in a box, a canonical example of quantum mechanics, and we present analytic and numerical investigations on this problem. After deriving an exact Volterra-type integral equation, composed of an infinite sum of modes, we show that approximate formulas with the lowest-frequency modes correctly capture the qualitative behavior of the wave function. If we take into account hundreds of modes, our numerical calculation shows that the quantum adiabatic theorem actually gives a very good approximation even if the barrier height diverges within finite time, as long as it is sufficiently longer than the characteristic time scale of the particle. In particular, if the barrier is slowly inserted at an asymmetric position, the particle is localized by the insertion itself, in accordance with a prediction of the adiabatic theorem. On the other hand, when the barrier is inserted quickly, the wave function becomes rugged after the insertion because of the energy transfer to the particle. Regardless of the position of the barrier, the fast insertion leaves the particle unlocalized so that we can obtain meaningful information by a which-side measurement. Our numerical procedure provides a precise way to calculate the wave function throughout the process, from which one can estimate the amount of this information for an arbitrary insertion protocol.

PACS numbers: 03.65.Ge,02.60.Cb,07.20.Pe

* seungki@pknu.ac.kr

I. INTRODUCTION

The “particle in a box” problem describes a localized particle in a deep potential well. It is one of the most basic problems in textbooks of quantum mechanics, yet relevant in many physical situations. In particular, the mathematical simplicity makes it a useful starting point to study many different phenomena, such as quantum dots [1], ideal gases [2], and energy bands in a periodic crystal lattice [3]. An important application of the particle in a box problem is the Szilard engine [4–6], which has drawn attention in the context of information thermodynamics [7–13]. The original Szilard engine is illustrated as a classical particle in a box, in the middle of which an impenetrable barrier is inserted to create uncertainty of one bit [14]. The uncertainty is resolved by measuring the position of the particle, and the resulting information can be used to extract work from a single thermal reservoir. After the work extraction, the barrier is removed from the box, which completes one cycle. Since the criticism on thermodynamics of the single-particle gas [15], however, it has been argued that the Szilard engine requires quantum-mechanical treatment [5]. Along this line, for example, one can model the working substance of the engine as a particle governed by the Schrödinger equation with a time-dependent potential barrier.

If we are to take into account the time dependence, one of the easiest ways would be to consider an infinitely slow protocol for changing the barrier height in an isolated system, to which the adiabatic theorem is applicable [16]. The occupation probabilities then remain unchanged while the energy levels are shifted. Another extreme case is to insert an infinitely high barrier all of sudden at time $t = 0$, which has been claimed to generate an unusual quantum state with a fractal wave function [17]. These two protocols bring the system out of equilibrium at the end of the process, at which isothermal expansion gets started. To avoid abrupt transitions at this moment, one may alternatively consider an isothermal process, throughout which the system evolves quasistatically in contact with a thermal reservoir [6, 18]. If the reservoir has very low temperature, however, this protocol runs into a trouble: The thermal contact always brings the system to the ground state. If the ground state is nondegenerate, it means that the system has no uncertainty so that no work can be extracted by the engine [18]. It happens when the barrier is off the middle of the box, which should always be the case in experiments.

Motivated by the quantum Szilard engine, we in this work calculate the time evolution

of a quantum particle in an isolated box when the δ -function barrier is inserted with a finite speed. This model deserves attention in its own right as a generalization of the particle in a box problem, because the Schrödinger equation is not explicitly solvable in the presence of a time-dependent potential except a few special cases [19–23]. It is also of experimental relevance in the context of splitting matter waves such as Bose-Einstein condensates [24–27]. This topic has been investigated over the past decade since the experimental realization of a stable double-well trap, which can be used for implementing an atom interferometer [28] or a Josephson junction [29]. Researchers have mostly considered deforming a harmonic trap to split a wave function, but it would also be experimentally feasible to localize a wave function inside a deep square potential well and split it with a sharp laser beam. The solution for a finite-speed protocol will be generally useful in the sense that it describes an experimentally accessible situation, whereas infinitely slow or fast protocols are only approximate to reality. Furthermore, if we are interested in the power of an engine in evaluating the performance [30–32], we must definitely consider a finite-speed protocol, and this work can provide a starting point in this direction as well.

A strategy to solve the Schrödinger equation with a time-dependent δ -function barrier is to convert it to a Volterra-type integral equation, as suggested by Ref. 33. We will demonstrate how this equation can be studied in a systematic way, in combination with analytic and numerical calculations. This work is organized as follows. In the next section, we derive the Volterra-type integral equation from the Schrödinger equation. Some approximate expressions will also be given there. In Sec. III, we present a numerical procedure to solve the integral equations and discuss the results. We then conclude this work in Sec. IV.

II. ANALYSIS

A. Formal solution

The Schrödinger equation is written in dimensionless units as

$$-\psi_{xx} + 2c(t)\delta(x - x_0)\psi = i\psi_t, \quad (1)$$

where the subscripts mean partial derivatives. The strength of the δ -function potential is controlled by $c(t)$, which is called a protocol in this work. Let us choose our initial condition

at $t = 0$ as the n th eigenstate $\phi_n(x)$ in the absence of the δ -function potential:

$$\psi(x, 0) = \phi_n(x) = \begin{cases} L^{-1/2} \cos nkx & \text{if } |x| < L \text{ and } n \text{ is odd,} \\ L^{-1/2} \sin nkx & \text{if } |x| < L \text{ and } n \text{ is even,} \\ 0 & \text{otherwise,} \end{cases} \quad (2)$$

where $k \equiv \pi/(2L)$ and $n = 1$ corresponds to the ground state. The particle is confined in a box ranging from $x = -L$ to $x = +L$, so that the boundary condition is given by $\psi(x, t) = 0$ at $x = \pm L$. If $-L < x < x_0$ or $x_0 < x < L$, we are back to the free space described by $-\psi_{xx} = i\psi_t$. We restrict ourselves to $t > 0$ and take the Laplace transform \mathcal{L} to obtain

$$\overline{\psi}_{xx} + is\overline{\psi} = i\psi(x, 0), \quad (3)$$

where $\overline{\psi}(x, s) \equiv \mathcal{L}[\psi(x, t)] = \int_0^\infty dt e^{-st} \psi(x, t)$ with $s > 0$. To solve the Schrödinger equation with a time-dependent potential, we transform it to an integral equation as suggested in Ref. 33. In Appendix A, we derive the following solution,

$$\overline{\psi}(x, s) = \frac{\phi_n(x)}{s + in^2k^2} + \mathcal{L}[c(t)\psi(x_0, t)]F(x, s), \quad (4)$$

where

$$F(x, s) = \begin{cases} \frac{(e^{2i\sqrt{is}L} - e^{2i\sqrt{is}x})(e^{2i\sqrt{is}(L+x_0)} - 1)}{i\sqrt{is}e^{i\sqrt{is}(x+x_0)}(e^{4i\sqrt{is}L} - 1)} & \text{for } x_0 \leq x < L, \\ \frac{(e^{2i\sqrt{is}L} - e^{2i\sqrt{is}x_0})(e^{2i\sqrt{is}(L+x)} - 1)}{i\sqrt{is}e^{i\sqrt{is}(x+x_0)}(e^{4i\sqrt{is}L} - 1)} & \text{for } -L < x < x_0. \end{cases} \quad (5)$$

In Appendix B, we perform the inverse Laplace transform to obtain

$$\psi(x, t) = \phi_n(x)e^{-in^2k^2t} + \sum_{\nu=1}^{\infty} \int_0^t dt' c(t') \psi(x_0, t') f_\nu(x, t-t'), \quad (6)$$

where

$$f_\nu(x, t) = \begin{cases} \frac{1}{2iL} e^{-i\nu^2k^2t - i\nu k(x+x_0)} [(-1)^\nu - e^{2i\nu kx}] [e^{2i\nu k(L+x_0)} - 1] & \text{for } x_0 < x < L \\ \frac{1}{2iL} e^{-i\nu^2k^2t - i\nu k(x+x_0)} [(-1)^\nu - e^{2i\nu kx_0}] [e^{2i\nu k(L+x)} - 1] & \text{for } -L < x < x_0. \end{cases} \quad (7)$$

Equation (6) has to be solved in two steps. First, we solve it for $x = x_0$ to get $\psi(x_0, t)$. The next step is to substitute $\psi(x_0, t)$ back into Eq. (6) to obtain $\psi(x, t)$. Note that $\psi(x_0, t)$ contains essential information of the full wave function in this formulation.

B. Insertion at the origin

To proceed, it is more convenient to deal with a specific situation. Suppose that the system is initially in the ground state, i.e., $\psi(x, 0) = \phi_1(x)$. If we insert the δ -potential barrier at the origin by setting $x_0 = 0$, Eq. (6) reduces to

$$\psi(x, t) = L^{-1/2} e^{-ik^2 t} \cos kx - 2iL^{-1} \sum_{\mu=0}^{\infty} \cos[(2\mu+1)kx] \int_0^t dt' c(t') \psi(0, t') e^{-i(2\mu+1)^2 k^2 (t-t')}. \quad (8)$$

We may express Eq. (8) as the cosine series

$$\psi(x, t) = L^{-1/2} \sum_{\mu=0}^{\infty} \sigma_{\mu}(t) \cos[(2\mu+1)kx], \quad (9)$$

with $\sigma_{\mu}(t) \equiv e^{-ik^2 t} \delta_{\mu 0} - 2iL^{-1/2} \int_0^t dt' c(t') \psi(0, t') e^{-i(2\mu+1)^2 k^2 (t-t')}$, where $\delta_{\alpha\beta}$ means the Kronecker δ . The conservation of total probability implies that

$$\sum_{\mu=0}^{\infty} |\sigma_{\mu}(t)|^2 = 1, \quad (10)$$

because $L^{-1} \int_{-L}^L dx \cos[(2\mu+1)kx] \cos[(2\mu'+1)kx] = \delta_{\mu\mu'}$ for integers μ and μ' . The total energy of the particle is obtained as

$$E(t) = \sum_{\mu=0}^{\infty} (2\mu+1)^2 k^2 |\sigma_{\mu}(t)|^2 + 2c(t) \left| \sum_{\mu=0}^{\infty} \sigma_{\mu}(t) \right|^2, \quad (11)$$

where the first and second terms represent the kinetic and potential parts, respectively.

1. Single-mode approximation

In our specific case described by Eq. (8), let us define

$$g(x, t; \mu) \equiv 2iL^{-1} \cos[(2\mu+1)kx] \int_0^t dt' c(t') \psi(0, t') e^{-i(2\mu+1)^2 k^2 (t-t')} \quad (12)$$

to rewrite Eq. (8) as

$$\psi(x, t) = L^{-1/2} e^{-ik^2 t} \cos kx - \sum_{\mu=0}^{\infty} g(x, t; \mu). \quad (13)$$

It is straightforward to obtain the following equality for the time derivative of g :

$$g_t(x, t; \mu) = [-i(2\mu+1)^2 k^2] g(x, t; \mu) + 2iL^{-1} c(t) \psi(0, t) \cos[(2\mu+1)kx]. \quad (14)$$

If we assume that only the lowest-frequency mode with $\mu = 0$ is dominant, Eq. (13) is simplified to

$$\psi(x, t) \approx L^{-1/2} e^{-ik^2 t} \cos kx - g(x, t; 0). \quad (15)$$

Taking the time derivative, we find that

$$\begin{aligned} \psi_t(x, t) &\approx L^{-1/2} (-ik^2) e^{-ik^2 t} \cos kx - (-ik^2) g(x, t; 0) - 2iL^{-1} c(t) \psi(0, t) \cos kx \\ &\approx L^{-1/2} (-ik^2) e^{-ik^2 t} \cos kx \\ &\quad - (-ik^2) [L^{-1/2} e^{-ik^2 t} \cos kx - \psi(x, t)] - 2iL^{-1} c(t) \psi(t) \cos kx \\ &= -ik^2 \psi(x, t) - 2iL^{-1} c(t) \psi(0, t) \cos kx, \end{aligned} \quad (16)$$

where we have used Eq. (15) to remove $g(x, t; 0)$. Rearranging the terms, we obtain the equation

$$\left(\frac{\partial}{\partial t} + ik^2 \right) \psi(x, t) \approx -2iL^{-1} c(t) \psi(0, t) \cos kx, \quad (17)$$

where the right-hand side (RHS) represents a ‘driving’ term due to the δ -potential barrier. If we regard $c(t)\psi(0, t)$ on the RHS as an external parameter, we can write the formal solution of the first-order ordinary differential equation (ODE) [34], which is identical to Eq. (15). As mentioned above, the evolution at the insertion point is most important in determining the full wave function in our formulation. At $x = 0$, we see from Eq. (16) that

$$\psi_t(0, t) \approx -i[k^2 + 2L^{-1}c(t)]\psi(0, t), \quad (18)$$

for which the solution is obtained as

$$\psi(0, t) \approx \psi(0, 0) \exp \left[-i \left(k^2 t + 2L^{-1} \int_0^t dt' c(t') \right) \right]. \quad (19)$$

The lowest-mode approximation thus describes an effect of $c(t)$ on the phase of $\psi(0, t)$ without altering the magnitude.

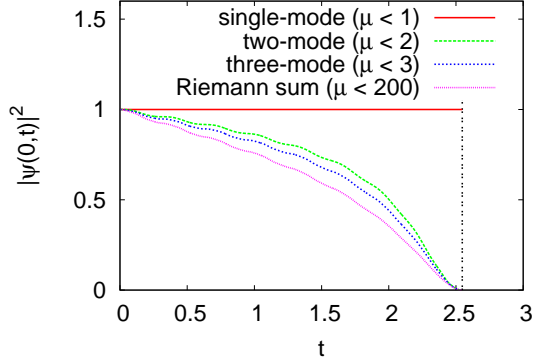


FIG. 1. (Color online) Probability density at $x = x_0 = 0$, when the particle is assumed to be in the ground state at $t = 0$. The protocol is chosen as $c(t) = \tan(k^2 t/4)$ with $L \equiv 1$. The vertical line represents $t^* = 2\pi/k^2 = 8/\pi \approx 2.55$, where the barrier height diverges to infinity. The single-mode approximation [Eq. (16)] does not describe the amplitude change, but the two-mode approximation is already plausible, and the result is further improved in the three-mode approximation. The Riemann sum means the calculation explained in Sec. III. We use the second-order Runge-Kutta method [35] to integrate the ODEs resulting from the two- and three-mode approximations such as Eq. (24).

2. Two-mode approximation

If we additionally take into account the next mode with $\mu = 1$, we find the following set of equations by taking time derivatives:

$$\psi(x, t) \approx L^{-1/2} e^{-ik^2 t} \cos kx - g(x, t; 0) - g(x, t; 1) \quad (20)$$

$$\begin{aligned} \psi_t(x, t) \approx & L^{-1/2} (-ik^2) e^{-ik^2 t} \cos kx \\ & - [(-ik^2)g(x, t; 0) + 2iL^{-1}c(t)\psi(0, t) \cos kx] \\ & - [(-9ik^2)g(x, t; 1) + 2iL^{-1}c(t)\psi(0, t) \cos 3kx] \end{aligned} \quad (21)$$

$$\begin{aligned} \psi_{tt}(x, t) \approx & L^{-1/2} (-ik^2)^2 e^{-ik^2 t} \cos kx \\ & - (-ik^2)[(-ik^2)g(x, t; 0) + 2iL^{-1}c(t)\psi(0, t) \cos kx] \\ & - 2iL^{-1}c_t(t)\psi(0, t) \cos kx - 2iL^{-1}c(t)\psi_t(0, t) \cos kx \\ & - (-9ik^2)[(-9ik^2)g(x, t; 1) + 2iL^{-1}c(t)\psi(0, t) \cos 3kx] \\ & - 2iL^{-1}c_t(t)\psi(0, t) \cos 3kx - 2iL^{-1}c(t)\psi_t(0, t) \cos 3kx. \end{aligned} \quad (22)$$

By using the first two equations, one can remove $g(x, t; 0)$ and $g(x, t; 1)$ in the last one to derive a second-order ODE for $\psi(x, t)$:

$$\begin{aligned} \left(\frac{\partial}{\partial t} + ik^2\right) \left(\frac{\partial}{\partial t} + 9ik^2\right) \psi(x, t) \approx & -2iL^{-1} \left(\frac{\partial}{\partial t} + ik^2\right) [c(t)\psi(0, t)] \cos kx \\ & -2iL^{-1} \left(\frac{\partial}{\partial t} + 9ik^2\right) [c(t)\psi(0, t)] \cos 3kx. \end{aligned} \quad (23)$$

The left-hand side (LHS) is related to the two lowest modes at $t = 0$, whereas the RHS represents the effect of the barrier interacting with the wave function at $x = 0$. Once again, the formal solution of Eq. (23) for given $c(t)\psi(0, t)$ should be identical to Eq. (20). At the insertion point $x = 0$, it yields the following equation with time-dependent coefficients:

$$\pi\psi_{tt}(0, t) + [10i\pi k^2 + 8ikc(t)]\psi_t(0, t) + [-9\pi k^4 - 40k^3c(t) + 8ikc_t(t)]\psi(0, t) \approx 0. \quad (24)$$

An advantage of this approximate formula is that $\psi(0, t)$ can be explicitly obtained in terms of the Hermite polynomial and the hypergeometric function for a simple protocol such as $c(t) \propto t$. However, the solution is not very illuminating, and, more importantly, such a linear protocol does not split the wave function within a finite time. So we will numerically integrate Eq. (24), by choosing the protocol as $c(t) = \tan(k^2t/4)$, which diverges to infinity at $t^* \equiv 2\pi/k^2 = 8L^2/\pi$. Starting from ground-state properties $\psi(0, 0) = 1$ and $\psi_t(0, 0) = -ik^2$ as the initial conditions, we see that Eq. (24) now describes amplitude changes as well (Fig. 1). In particular, the approximation predicts that the probability density $|\psi(0, t)|^2$ vanishes as t approaches t^* , which is physically reasonable. It is also plausible that the approximation can be improved systematically by including more and more modes, and the number of included modes will correspond to the order of the resulting ODE to integrate. In the next section, we present a numerical method based on the Riemann sum, by which one can carry out the summation of Eq. (13) over $\mu \lesssim O(10^2)$. Figure 1 shows that the results with a few lowest modes are not very far apart from it. We have so far discussed one way to use Eq. (24), i.e., starting from $c(t)$ to obtain $\psi(0, t)$ and then proceed to $\psi(x, t)$. We may also consider the opposite direction; that is, let us start from the desired evolution of $\psi(x, t)$, from which $\psi(0, t)$ is obtained. If Eq. (24) is solved for $c(t)$ with this $\psi(0, t)$, the result is the following (Appendix C):

$$c(t) \approx \frac{iLe^{-5ik^2t}}{4\psi(0, t)} \int_0^t dt' e^{5ik^2t'} \left(\frac{\partial}{\partial t'} + ik^2\right) \left(\frac{\partial}{\partial t'} + 9ik^2\right) \psi(0, t') + \frac{c(0)\psi(0, 0)}{\psi(0, t)} e^{-5ik^2t}. \quad (25)$$

Equation (25) suggests that one can design the protocol $c(t)$ to guide the evolution of $\psi(x, t)$ within the two-mode approximation. If $\psi(0, t)$ stays at one of the two lowest eigenmodes, for example, the first term of Eq. (25) identically vanishes and we find that $c(t) \approx \frac{c(0)\psi(0,0)}{\psi(0,t)}e^{-5ik^2t}$. If $c(t) \neq 0$, one might reach a conclusion that $\psi(0, t) \propto e^{-5ik^2t}$, considering that $c(t)$ must be real for any t . This is self-contradictory, however, because no eigenmode has phase velocity $-5k^2$. The only possibility is to set $c(t) = 0$. As a more nontrivial example, let us write $\psi(0, t) = A(t)e^{i\varphi(t)}$ and suppose that the amplitude decays as $A(t) = A_0e^{-\lambda t}$ with real positive constants A_0 and λ . The phase $\varphi(t)$ is a real number in $(-\infty, +\infty)$. Substituting this $\psi(0, t)$ into Eq. (24), we obtain the following set of equations:

$$\pi\varphi_t^2 + [10\pi k^2 + 8kc(t)]\varphi_t + 9\pi k^4 + 40k^3c(t) - \pi\lambda^2 = 0 \quad (26)$$

$$\pi\varphi_{tt} + 2\pi\lambda\varphi_t - 10\pi\lambda k^2 - 8\lambda kc(t) + 8kc_t(t) = 0. \quad (27)$$

Equation (26) is quadratic in φ_t and can be solved as

$$\varphi_t = \frac{1}{2\pi} \left\{ -[10\pi k^2 + 8kc(t)] \pm \sqrt{64\pi^2 k^4 + 64k^2 c^2(t) + 4\pi^2 \lambda^2} \right\}, \quad (28)$$

where we will choose the plus sign to have $\lim_{\lambda \rightarrow 0} \varphi_t = -k^2$ on the ground state. By plugging Eq. (28) into Eq. (27), one derives a nonlinear differential equation for $c(t)$. It can be linearized by keeping only linear terms in λ and $c(t)$, which results in $c(t) \approx \frac{3\pi k}{4}(e^{4\lambda t} - 1) \approx 3\pi k\lambda t$. To sum up, if we choose how the amplitude changes over time, it determines the evolution of the phase, due to the constraint that $c(t)$ must be real. By combining these $A(t)$ and $\varphi(t)$, it is possible to construct $c(t)$. Note that the phase velocity φ_t in Eq. (28) converges to $-5k^2$ as $c(t) \rightarrow \infty$. This value turns out to be an average of $-k^2$ and $-9k^2$, which are for the first and second modes, respectively, and a little different from the phase velocity of the first excited state, $-4k^2$, in this two-mode approximation.

III. NUMERICAL CALCULATION

Numerical calculation can be a useful tool to explore Eq. (6), as we will show in this section. Throughout this section, we will use the same protocol $c(t) = \tan(k^2 t/4)$ as in the above example. Recall that the box is completely separated into two subsystems at $t = t^* = 2\pi/k^2$, so that we have to only consider $t \in [0, t^*)$. Our numerical strategy is to divide this time interval into M pieces to use the left Riemann sum for the integral over t'

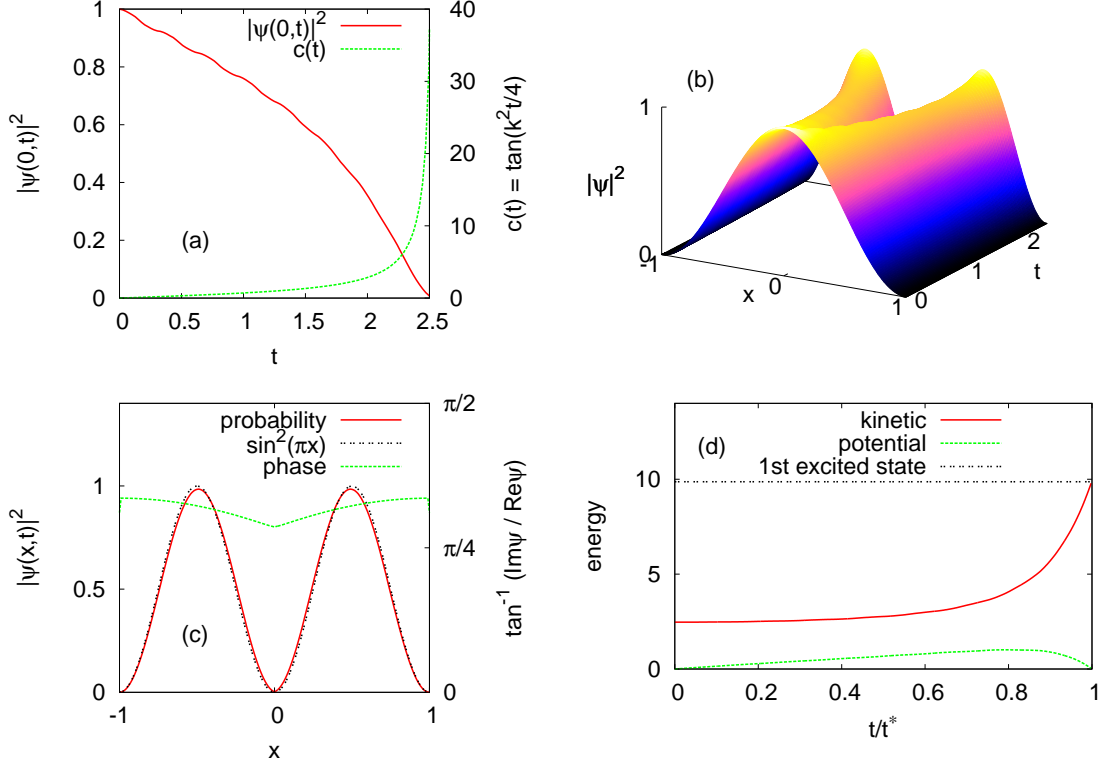


FIG. 2. (Color online) Numerical result of probability density $|\psi(x,t)|^2$ from an initial condition specified by Eq. (A7) with $L \equiv 1$. The δ potential grows as $c(t) = \tan(k^2 t/4)$ at the origin and diverges as $t \rightarrow t^* = 2\pi/k^2 = 8/\pi \approx 2.55$. (a) Probability density at the origin as a function of time, together with $c(t)$ for comparison. (b) Full shape of $|\psi(x,t)|^2$. (c) Probability density and phase at time $t = 0.99 \times t^*$ (solid). The black dotted line shows the probability density of the first excited state, $\sin^2(\pi x)$, for comparison. (d) Energy of the particle. The horizontal line indicates the energy of the first excited state.

in Eq. (8). It is convenient to define

$$F_\mu(t) \equiv \int_0^t dt' c(t') \psi(0, t') e^{i(2\mu+1)^2 k^2 t'}, \quad (29)$$

and approximate it as

$$F_\mu(T\epsilon) \approx \epsilon \sum_{l=0}^{T-1} c(l\epsilon) \psi(0, l\epsilon) e^{i(2\mu+1)^2 k^2 l\epsilon}, \quad (30)$$

where we have identified dt and t with ϵ and $T\epsilon$, respectively, by introducing an integer $T \in (0, M)$ and $\epsilon \equiv t^*/M$. At the next time step, F_μ is updated as follows:

$$F_\mu(T\epsilon + \epsilon) = F_\mu(T\epsilon) + \epsilon c(T\epsilon) \psi(0, T\epsilon) e^{i(2\mu+1)^2 k^2 T\epsilon}. \quad (31)$$

We obtain $\psi(0, T\epsilon)$ by calculating

$$\psi(0, T\epsilon) \approx L^{-1/2} e^{-ik^2 T\epsilon} - \frac{2i}{L} \sum_{\mu=0}^N F_{\mu}(T\epsilon) e^{-i(2\mu+1)^2 k^2 T\epsilon} \quad (32)$$

with $N \gg 1$ to include a sufficiently large number of modes. At the same time, it is worth noting that $(2N + 1)^2 \epsilon$ must be small enough to perform the integration in Eq. (29). By iterating Eqs. (31) and (32), we can get $\psi(0, t)$ within the time interval $[0, t^*)$ [Fig. 2(a)]. Note that Fig. 1 has already shown the curve of $|\psi(0, t)|^2$ obtained in this way to compare it with the two- and three-mode approximations. We compute $\psi(x, T\epsilon)$ for nonzero x in a similar manner, because Eq. (8) is discretized as

$$\psi(x, T\epsilon) \approx L^{-1/2} e^{-ik^2 T\epsilon} \cos kx - \frac{2i}{L} \sum_{\mu=0}^N F_{\mu}(T\epsilon) e^{-i(2\mu+1)^2 k^2 T\epsilon} \cos[(2\mu + 1)kx]. \quad (33)$$

Although we have discussed $x_0 = 0$ for brevity, the generalization to $x_0 \neq 0$ is straightforward. An advantage of this approach is that Eq. (33) can be computed in parallel for many different x 's. In this way, one can get the full shape of the probability density $|\psi(x, t)|^2$ as depicted in Fig. 2(b). Figure 2(c) shows $|\psi(x, t)|^2$ at $t = 0.99 \times t^*$ in comparison with $\sin^2(\pi x/L)$, the probability density of the first excited state. We have assured ourselves that the normalization condition [Eq. (10)] is satisfied within the accuracy of 10^{-3} throughout the calculation. Figure 2(d) shows the kinetic and potential energies of the particle as functions of time [Eq. (11)]. As t approaches t^* , the total energy converges to $4k^2$, the energy of the first excited state $\phi_2(x)$. As can be seen from Eq. (9), however, $\psi(x, t)$ must be symmetric with respect to the origin, so we conclude that $\psi(x, t^*) \propto |\sin(2kx)|$ to a good approximation.

Even if this is expected in the limit of the adiabatic theorem [16], it is not obvious *a priori* when the barrier is inserted within finite time. A qualitative explanation goes as follows: The energy level spacing between the ground and first excited states amounts to $3\pi^2/4 \approx 7.40$ at $t = 0$ in our units. The characteristic time scale will thus be of $O(4/3\pi^2) \sim O(10^{-1})$, which is roughly 5% of the total time $t^* \approx 2.55$ to insert the barrier. For this reason, we can still say that the insertion is relatively slow. This argument can be made more quantitative by approximating our particle as a two-level system consisting of the ground state and the first excited state. Such approximation is reasonable, because other excited states are very far away from these two in the energy spectrum. According to the Landau-Zener formula,

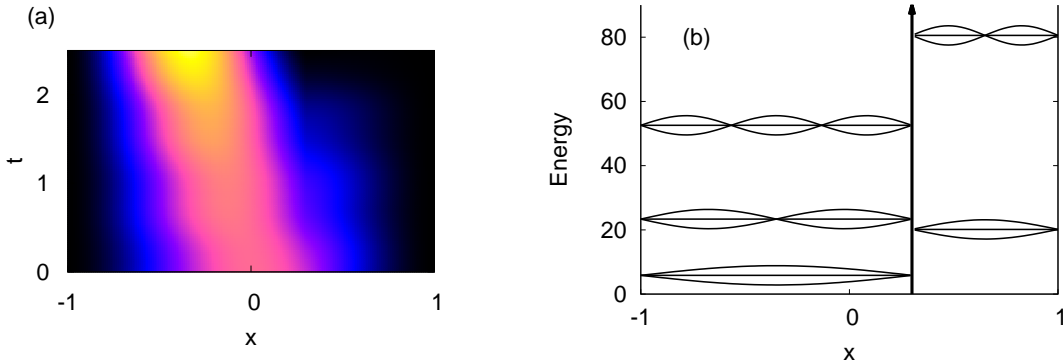


FIG. 3. (Color online) Time evolution of $|\psi(x,t)|^2$ when the barrier is inserted at $x_0 = 0.3$. (a) If the initial condition is the ground state, i.e., $\psi(x,0) = \phi_1(x) = \cos kx$, the particle will be localized on the left side of the box in the end. (b) Energy levels in the two subsystems separated by the barrier at $x_0 = 0.3$, represented by the upward arrow. The ground state of the total system is found on the left side.

if the energy levels approach to each other with speed $\dot{\Delta}$, the occupation probability P_2 of the first excited state will be estimated by $\ln(P_2) \propto -\dot{\Delta}^{-1}$ at the end of the protocol. If $\dot{\Delta} \ll 1$, therefore, the system will remain in the ground state with high probability, which is the case when t is roughly less than $0.8 t^*$ in Fig. 2(a). The rapid increase of the barrier height for $t \gtrsim 0.8 t^*$ just gently pushes the particle out of the origin, because the probability density at the origin has already become low at $t = 0.8 t^*$. As a result, the particle is mostly preserved in the ground state.

If the wall is away from the origin, i.e., $x_0 \neq 0$, the particle can be localized at $t = t^*$ on the wider side of the box [36, 37]. For example, Fig. 3(a) shows the case of $x_0 = 0.3$. This is also easily explained by applying the adiabatic theorem: Let $L_1 = L + x_0$ denote the size of this wider side, whereas $L_2 = L - x_0$ denotes that of the other side. The ground state at $t = t^*$ has nonzero probability only on the wider side of the box with an energy level $E_1 = \pi^2/L_1^2$ [Fig. 3(b)]. The energy on the narrower side, $E_2 = \pi^2/L_2^2$ is more than three times higher than this ground-state energy. When the energy-level spacing is so large, our protocol can preserve the most part of the system in the ground state. We thus need only a single energy eigenstate to confine the particle on one side of the box at $t = t^*$ if the barrier is slowly inserted at an asymmetric position. In other words, the which-side measurement commutes with the Hamiltonian of this system in the quasistatic limit. However, when the

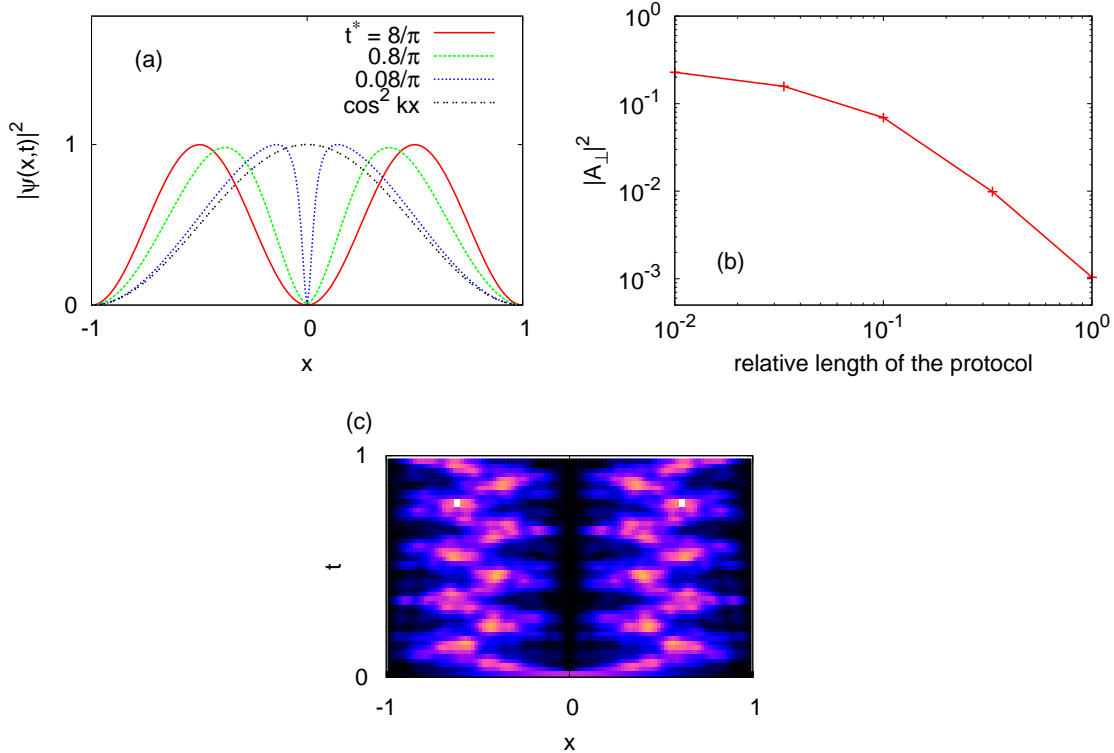


FIG. 4. (Color online) Insertion of the barrier at $x_0 = 0$ in a box with $L = 1$. The wave function is initially in the ground state, i.e., $\psi(x, 0) = \phi_1(x) = \cos kx$. (a) Probability densities for various insertion speeds, when the wave function is split into two parts. We have also plotted the initial probability density function $|\psi(x, 0)|^2 = |\phi_1(x)|^2 = \cos^2 kx$ for comparison. (b) Differences from the adiabatic limit (see text) near the end of the protocol. On the horizontal axis, the unit length of the protocol is defined by $8/\pi \approx 2.55$. (c) The time evolution of $|\psi(x, t)|^2$ in case of the fastest insertion with $t^* = 0.08/\pi$. The wave function for $t > t^*$ is obtained by using the spectral method [35].

protocol is fast enough compared with the energy gap, we can no longer neglect excitation, and this creates uncertainty to be resolved by a which-side measurement.

We have thus confirmed that our calculation produces physically reasonable results as long as the process is slow enough with respect to the characteristic time scale of the system. Obviously, our numerical calculation is not restricted to such a slow protocol, and we can also check what happens if we speed up the insertion. It is clear that the wave function will not converge to the ground state of the subsystem any more but occupy higher energy levels at the end of the process. Our calculation makes this guess more precise: Figure 4(a)

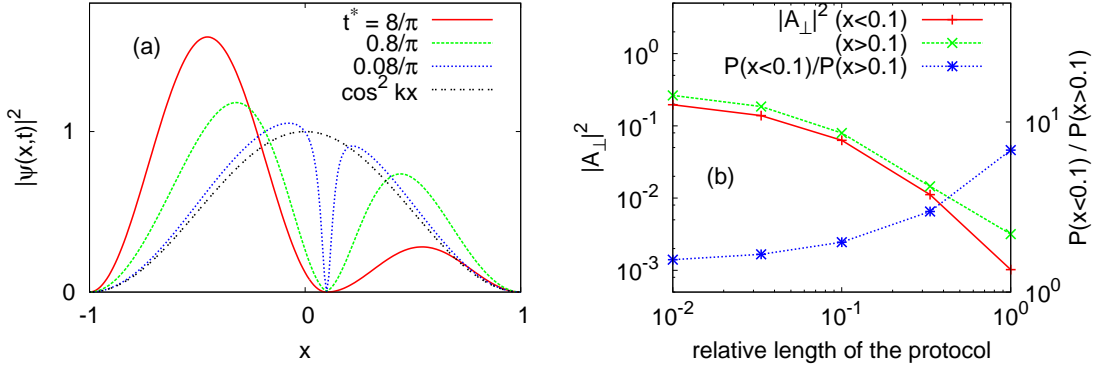


FIG. 5. (Color online) Evolution of the wave function for various insertion speeds, when the barrier is inserted at $x_0 = 0.1$. Except x_0 , the other parameters are the same as in Fig. 4. (a) Probability densities after the split, plotted with the initial probability density function $|\psi(x, 0)|^2 = |\phi_1(x)|^2 = \cos^2 kx$ for comparison. (b) Difference from the adiabatic limit on the two sides of the box at $t \approx t^*$. On the vertical secondary axis, we have also shown the ratio of the probability to find the particle at $x < 0.1$ to that of $x > 0.1$.

shows the probability densities at $t \approx t^*$, and we have checked various t^* across two orders of magnitude. The case of $t^* = 0.08/\pi$ describes a situation in which the insertion speed is much faster in comparison to the characteristic time scale of the system $\sim O(10^{-1})$. As a consequence, the overall shape at the end of the protocol does not deviate much from the starting point, $|\psi(x, 0)|^2 = |\phi_1(x)|^2 = L^{-1} \cos^2 kx$. As mentioned above, we expect $\psi(x, t) \rightarrow \psi_{\parallel}(x) \equiv L^{-1/2} |\sin 2kx|$ in the adiabatic limit up to a phase factor. We thus decompose $\psi(x, t)$ into parallel and perpendicular components to $\psi_{\parallel}(x, t)$ as

$$\psi(x, t) = A_{\parallel} \psi_{\parallel}(x, t) + A_{\perp} \psi_{\perp}(x, t), \quad (34)$$

where $\psi_{\perp}(x, t)$ is a normalized wave function perpendicular to $\psi_{\parallel}(x, t)$. The normalization condition of $\psi(x, t)$ requires that $|A_{\parallel}|^2 + |A_{\perp}|^2 = 1$. In Fig. 4(b), we plot $|A_{\perp}|^2$ with varying the length of the protocol, measured in units of $8/\pi$. As we slow down the insertion, the difference from the adiabatic limit decreases drastically. This point is especially important in splitting a wave function within a finite time [24–27]. In case of a quick protocol, the excitation to higher-energy modes, as manifested by the dip around the origin, makes the wave function rugged in further time evolution [Fig. 4(c)]. We note that this result is consistent with the predicted fractal wave function [17]. Even if $x_0 \neq 0$, the excitation

makes both sides of the box occupied, creating uncertainty to be resolved by a which-side measurement [Fig. 5(a)]. Differently from the quasistatic protocol, therefore, we can still make use of the information to extract work with a finite-time protocol. Our numerical procedure provides a precise way to obtain the wave function, from which the amount of uncertainty can be estimated. Figure 5(b) depicts the trade-off between the uncertainty and the excitation to other eigenmodes. This is crucial in the context of splitting a matter wave, where it is desirable to keep the uncertainty while minimizing excitation at the same time. Figure 5(b) shows that the excitation can be suppressed with $|A_{\perp}|^2 \lesssim O(10^{-2})$, while the asymmetry of probabilities are also kept less than $O(10)$, if $t^* \approx 8/\pi$ for $x_0 = 0.1$.

IV. DISCUSSION AND SUMMARY

In summary, we have investigated a quantum particle in an isolated box with a time-dependent δ potential. We have found an integral expression for the wave function [Eq. (6)] together with an approximate formula [Eq. (24)]. The numerical evaluation through the integral equation gives precise results for the wave function during the barrier insertion, even if the process is completed within finite time. The total duration of the process, denoted by t^* , can be either short or long compared to the characteristic time scale of the particle, and the insertion point can be either symmetric or asymmetric. For all the cases considered, our numerical calculation has produced physically reasonable results in the light of the Landau-Zener formula.

In the context of splitting a wave function, we may consider a Bose-Einstein condensate in an optical trap forming a one-dimensional box [38–40]. The δ potential barrier can be implemented experimentally by shining a sharp laser beam onto the condensate. If the barrier height is increased with a sufficiently slow rate compared to the internal time scale of the system, the adiabatic limit can be reproduced with good accuracy [Fig. 4(b)]. In addition, we have also considered how to design the protocol within the two-mode approximation [Eqs. (26) and (27)]. If the barrier is off the middle of the box, its insertion localizes the wave function on one side of the box, instead of splitting it, in the adiabatic limit. This trade-off has been illustrated for $x_0 = 0.1$ in Fig. 5(b) so that one can choose the insertion speed based on the calculation.

If we return to the Szilard engine, the insertion of the barrier is followed by measuring

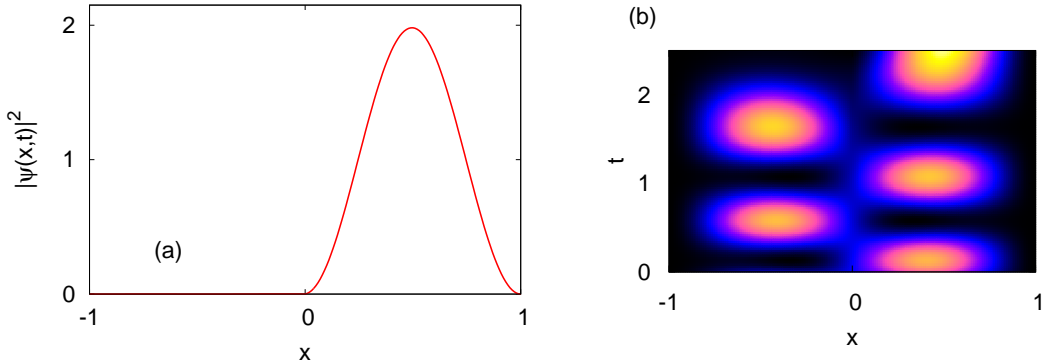


FIG. 6. (Color online) (a) Probability density of Eq. (35). at $t = 0.99t^*$ when t_0 is suitably chosen. (b) Time evolution of $|\Psi(x, t)|^2$ with the same t_0 .

the position of the particle and expanding this single-particle gas isothermally. Thereafter, the barrier should be removed to complete one cycle. As long as the engine can be treated as isolated from the environment, the removal of the barrier can be studied in the same way as in this work: It boils down to the derivation of an integral equation similar to Eq. (6), beginning with a localized initial condition due to the measurement. Instead of starting from scratch, however, we point out that our results in the previous section can be directly used to study the removal process in certain cases. For example, suppose that the wave function is described in the form

$$\Psi(x, t) = \frac{1}{\sqrt{2}} [\psi(x, t) + \phi_2(x, t)], \quad (35)$$

where $\psi(x, t)$ is obtained from Eq. (9) and $\phi_2(x, t)$ is the first excited state including time dependence. We may write it as $\phi_2(x, t) = \phi_2(x) e^{-4ik^2(t-t_0)}$ with certain reference time t_0 . It is obvious that $\phi_2(x, t)$ is not affected by the barrier, because the barrier is located at a node of this wave function. We also note that $\psi(x, t)$ and $\phi_2(x, t)$ are orthogonal to each other, because one is even and the other is odd with respect to $x \rightarrow -x$. By choosing a suitable t_0 for $\phi_2(x, t)$, we can induce destructive interference on the left side of the box at $t \approx t^*$, which effectively confines the particle to the right half of the box [Fig. 6(a)]. With this t_0 , we can also obtain the full time evolution of $\Psi(x, t)$ from $t = 0$ to $t \approx t^*$ [Fig. 6(b)]. If we define $\Psi^T(x, t) \equiv \overline{\Psi}(x, t^* - t)$, where the overbar means complex conjugate, it satisfies the following equation:

$$-\Psi_{xx}^T + 2c(t^* - t)\delta(x - x_0)\Psi^T = i\Psi_t^T. \quad (36)$$

Comparing this with the original Schrödinger equation [Eq. (1)], we see that $\Psi^T(x, t)$ solves the case of time reversal. Therefore, if we remove the barrier, the probability density will evolve from the top to the bottom in Fig. 6(b), because $|\Psi^T(x, t)|^2 = |\Psi(x, t^* - t)|^2$. We clearly observe tunneling of the particle, resulting from a beat phenomenon between $\psi(x, t)$ and $\phi_2(x, t)$ [41], as the height of the barrier decreases. Such a beat phenomenon is weakened when the barrier is off the origin, because a single eigenstate is enough to localize a particle [Fig. 3(a)].

Considering that the quantum Szilard engine designed in Ref. 6 always keeps the quantum gas isothermal, it is fair to say that our computational framework can only hint at low-temperature behavior at best, because it deals with an isolated system. To understand the performance of a quantum information engine working at a finite temperature, we need to take into consideration a thermal reservoir in the quantum-mechanical context. That is far beyond the scope of the present work and will be undertaken in a future study.

ACKNOWLEDGMENTS

We gratefully acknowledge discussions with Sang Wook Kim. This work was supported by the Basic Science Research Program through the National Research Foundation of Korea (NRF), funded by the Ministry of Science, ICT and Future Planning (Grant No. NRF-2014R1A1A1003304).

Appendix A: Laplace transform of the Schrödinger equation

In the main text, we have written the Schrödinger equation through the Laplace transform as follows:

$$\bar{\psi}_{xx} + is\bar{\psi} = i\psi(x, 0). \quad (\text{A1})$$

The homogeneous equation in the absence of the RHS is solved by

$$\bar{\psi}_c(x, s) = a(s)y_1(x) + b(s)y_2(x), \quad (\text{A2})$$

where $y_1(x) \equiv e^{i\sqrt{is}x}$ and $y_2(x) \equiv e^{-i\sqrt{is}x}$. The prefactors $a(s)$ and $b(s)$ are determined by the boundary condition. The particular solution can be found by the integral

$$\bar{\psi}_p(x, s) = -y_1(x) \int dx' \frac{y_2(x')i\psi(x', 0)}{W(x)} + y_2(x) \int dx' \frac{y_1(x')i\psi(x', 0)}{W(x)}, \quad (\text{A3})$$

where W is the Wronskian of y_1 and y_2 :

$$W = \begin{vmatrix} y_1 & y_2 \\ y_1' & y_2' \end{vmatrix} = \begin{vmatrix} e^{i\sqrt{is}x} & e^{-i\sqrt{is}x} \\ i\sqrt{is}e^{i\sqrt{is}x} & -i\sqrt{is}e^{-i\sqrt{is}x} \end{vmatrix} = -2i\sqrt{is}. \quad (\text{A4})$$

The solution of Eq. (3) is given as $\bar{\psi}(x, s) = \bar{\psi}_c(x, s) + \bar{\psi}_p(x, s)$. More specifically, $\psi_p(x, s)$ can be expressed as

$$\bar{\psi}_p(x, s) = \int_{-\infty}^x dx' \frac{e^{i\sqrt{is}(x-x')}}{2\sqrt{is}} \psi(x', 0) - \int_{\infty}^x dx' \frac{e^{i\sqrt{is}(x'-x)}}{2\sqrt{is}} \psi(x', 0) \quad (\text{A5})$$

$$= \int_{-\infty}^{\infty} dx' \frac{e^{i\sqrt{is}|x-x'|}}{2\sqrt{is}} \psi(x', 0). \quad (\text{A6})$$

For example, suppose that we choose the ground state as our initial condition:

$$\psi(x, 0) = \begin{cases} L^{-1/2} \cos kx & \text{if } |x| < L, \\ 0 & \text{otherwise,} \end{cases} \quad (\text{A7})$$

where $k \equiv \pi/(2L)$. The particular solution is then explicitly given as

$$\bar{\psi}_p(x, s) = \frac{\sqrt{\frac{ik^2}{sL}} e^{i\sqrt{is}L} \cos(\sqrt{is}x) + L^{-1/2} \cos kx}{s + ik^2}. \quad (\text{A8})$$

We can carry out a similar integral to get an explicit expression for $\bar{\psi}_p(x, s)$ by choosing our initial condition as the n th eigenstate $\phi_n(x)$ in the absence of the δ -function potential

$$\psi(x, 0) = \phi_n(x) = \begin{cases} L^{-1/2} \cos nkx & \text{if } |x| < L \text{ and } n \text{ is odd,} \\ L^{-1/2} \sin nkx & \text{if } |x| < L \text{ and } n \text{ is even,} \\ 0 & \text{otherwise,} \end{cases} \quad (\text{A9})$$

where $n = 1$ corresponds to the ground state. To sum up, Eq. (3) has a solution of the following form:

$$\bar{\psi}(x, s) = \begin{cases} a_+ e^{i\sqrt{is}x} + b_+ e^{-i\sqrt{is}x} + \bar{\psi}_p(x, s) & \text{if } x > x_0, \\ a_- e^{i\sqrt{is}x} + b_- e^{-i\sqrt{is}x} + \bar{\psi}_p(x, s) & \text{if } x < x_0. \end{cases} \quad (\text{A10})$$

In addition, we have four conditions to determine the coefficients a_{\pm} and b_{\pm} :

$$\lim_{x \rightarrow x_0^+} \bar{\psi}(x, s) = \lim_{x \rightarrow x_0^-} \bar{\psi}(x, s), \quad (\text{A11})$$

$$\bar{\psi}(+L, s) = 0, \quad (\text{A12})$$

$$\bar{\psi}(-L, s) = 0, \quad (\text{A13})$$

$$\lim_{x \rightarrow x_0^+} \bar{\psi}_x(x, s) - \lim_{x \rightarrow x_0^-} \bar{\psi}_x(x, s) = 2c(t)\psi(x_0, t). \quad (\text{A14})$$

Note that the existence of the barrier inside the box is manifested by the last boundary condition at $x = x_0$ [Eq. (A14)]. One technical remark is in order: When one solves the Schrödinger equation with a time-varying potential, it is also common to use the coupled-channel method, which is perturbative expansion with the eigenmodes of the original barrier-free system [36]. However, the singular property of the δ function has led us to treat the time-varying potential as a boundary condition, as expressed in Eq. (A14). After some algebra, the solution is obtained as

$$\bar{\psi}(x, s) = \frac{\phi_n(x)}{s + in^2k^2} + \mathcal{L}[c(t)\psi(x_0, t)]F(x, s), \quad (\text{A15})$$

where

$$F(x, s) = \begin{cases} \frac{(e^{2i\sqrt{is}L} - e^{2i\sqrt{is}x})(e^{2i\sqrt{is}(L+x_0)} - 1)}{i\sqrt{is}e^{i\sqrt{is}(x+x_0)}(e^{4i\sqrt{is}L} - 1)} & \text{for } x_0 \leq x < L, \\ \frac{(e^{2i\sqrt{is}L} - e^{2i\sqrt{is}x_0})(e^{2i\sqrt{is}(L+x)} - 1)}{i\sqrt{is}e^{i\sqrt{is}(x+x_0)}(e^{4i\sqrt{is}L} - 1)} & \text{for } -L < x < x_0, \end{cases} \quad (\text{A16})$$

which is the result in the main text.

If we choose a linear protocol such as $c(t) = c_0t$ with a real constant c_0 , the second term on the RHS of Eq. (4) has an explicit form because $\mathcal{L}[t \times \psi(x_0, t)] = -\frac{d}{ds}\bar{\psi}(x_0, s)$ [33]. For $x = x_0$, therefore, we get a first-order ODE,

$$\bar{\psi}(x_0, s) = \frac{\phi_n(x_0)}{s + in^2k^2} - c_0 \frac{d}{ds}\bar{\psi}(x_0, s)F(x_0, s), \quad (\text{A17})$$

whose formal solution is always available [34]. For example, suppose that the particle occupies the ground state at $t = 0$, i.e., $n = 1$. If the barrier is inserted at $x_0 = 0$, we find that

$$\frac{d}{ds}\bar{\psi}(0, s) - c_0^{-1}\sqrt{is} \cot(\sqrt{is}L)\bar{\psi}(0, s) = -c_0^{-1} \frac{L^{-1/2}\sqrt{is} \cot(\sqrt{is}L)}{s + in^2k^2}. \quad (\text{A18})$$

The formal solution is thus written as

$$\bar{\psi}(0, s) = -c_0^{-1}e^{-I(s)} \int_0^s \frac{L^{-1/2}\sqrt{is'} \cot(\sqrt{is'}L)}{s' + in^2k^2} e^{I(s')} ds' + \bar{\psi}(0, 0)e^{-I(s)}, \quad (\text{A19})$$

where

$$\begin{aligned} I(s) &\equiv -c_0^{-1} \int_0^s \sqrt{is'} \cot(\sqrt{is'}L) ds' \\ &= \frac{2}{3}(is)^{3/2} + 2sL^{-1} \ln(1 - e^{-2i\sqrt{is}L}) + 2L^{-2}\sqrt{is}\text{Li}_2(e^{-2i\sqrt{is}L}) \\ &\quad - iL^{-3}\text{Li}_3(e^{-2i\sqrt{is}L}) + iL^{-3}\zeta(3). \end{aligned} \quad (\text{A20})$$

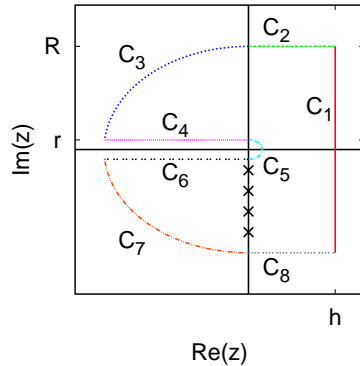


FIG. 7. (Color online) Keyhole contour to carry out the Bromwich integral [Eq. (B1)]. The crosses on the imaginary axis represent the poles of the integrand. The parameter h is a positive number, which is kept constant even when the radius R of C_3 and C_7 grows to infinity. At the same time, the radius of C_5 , denoted as r , approaches zero.

Note that Li_n is the polylogarithm function of order n , and ζ is the Riemann ζ function. The next step would be to use the solution $\bar{\psi}(x_0, s)$ to derive the full wave function $\bar{\psi}(x, s)$. Although the above procedure is formally exact, it is too complicated to obtain the wave function in the (x, t) space. In addition, we are more interested in a general protocol, which may go up to infinity within finite time. For this reason, we do not take this direction but directly apply the inverse Laplace transform to Eq. (4) as shown in the main text.

Appendix B: Inverse Laplace transform of Eq. (4)

Here, we consider the inverse Laplace transform of Eq. (4). It is elementary to transform the first term on the RHS of Eq. (4), because $\mathcal{L} \left[e^{-in^2k^2t} \right] = \frac{1}{s+in^2k^2}$. To use the convolution theorem for the second term, we need the inverse Laplace transform of $F(x, s)$ through the Bromwich integral [34]

$$\mathcal{L}^{-1} [F(x, s)] = \frac{1}{2\pi i} \int_{h-i\infty}^{h+i\infty} F(x, z) e^{zt} dz, \quad (\text{B1})$$

where $t > 0$. Equation (5) has simple poles on the imaginary axis at $z = -i\nu^2k^2$ with $\nu = 1, 2, \dots$, which implies that h can be an arbitrary positive constant. Let us consider a keyhole contour, as depicted in Fig. 7, with taking the negative real axis as a branch cut. The first path C_1 goes from $h - iR$ to $h + iR$. If R grows to infinity while h is kept constant,

the integral along C_1 is directly related to Eq. (B1). In such a limiting process, the length of C_2 remains constant, whereas the integrand decreases as $R^{-1/2}$. Therefore, we conclude that the integral along C_2 vanishes as $R \rightarrow \infty$, and the same conclusion holds for C_8 . Both C_3 and C_7 are ghost contours, because $|e^{zt}| = |e^{Rt \cos \theta}|$ and $\cos \theta$ is negative for $\theta \in (-\pi, \pi)$. One can also readily see that the integral along C_5 can be made arbitrarily small by taking the radius $r \rightarrow 0$. The remaining parts are C_4 and C_6 . Let us assume $x_0 < x < L$, because there is little difference for $-L < x < x_0$. Let X denote $\text{Re}(z)$. We have $z = e^{i\pi} X = -X$ and $\sqrt{z} = e^{i\frac{\pi}{2}} \sqrt{X} = i\sqrt{X}$ along C_4 , whereas $z = e^{-i\pi} X = X$ and $\sqrt{z} = e^{-i\frac{\pi}{2}} \sqrt{X} = -i\sqrt{X}$ along C_6 . Then, Eq. (5) gives us the integrands

$$F(x, z)|_{C_4} = \frac{\left(e^{-2\sqrt{iX}L} - e^{-2\sqrt{iX}x} \right) \left(e^{-2\sqrt{iX}(L+x_0)} - 1 \right)}{-\sqrt{iX} e^{-\sqrt{iX}(x+x_0)} \left(e^{-4\sqrt{iX}L} - 1 \right)}, \quad (\text{B2})$$

and

$$F(x, z)|_{C_6} = \frac{\left(e^{2\sqrt{iX}L} - e^{2\sqrt{iX}x} \right) \left(e^{2\sqrt{iX}(L+x_0)} - 1 \right)}{\sqrt{iX} e^{\sqrt{iX}(x+x_0)} \left(e^{4\sqrt{iX}L} - 1 \right)}. \quad (\text{B3})$$

A little algebra shows that Eqs. (B2) and (B3) are actually identical. The integrals along C_4 and C_6 are in the opposite directions, and therefore cancel out each other. Now we have evaluated the integral around the whole keyhole contour, and the residue theorem gives us $f_\nu(x, t)$ for each pole as follows:

$$f_\nu(x, t) = \begin{cases} \frac{1}{2iL} e^{-i\nu^2 k^2 t - i\nu k(x+x_0)} \left[(-1)^\nu - e^{2i\nu kx} \right] \left[e^{2i\nu k(L+x_0)} - 1 \right] & \text{for } x_0 < x < L \\ \frac{1}{2iL} e^{-i\nu^2 k^2 t - i\nu k(x+x_0)} \left[(-1)^\nu - e^{2i\nu kx_0} \right] \left[e^{2i\nu k(L+x)} - 1 \right] & \text{for } -L < x < x_0. \end{cases} \quad (\text{B4})$$

One might therefore conclude that $\mathcal{L}^{-1}[F(x, s)] = \sum_{\nu=1}^{\infty} f_\nu(x, t)$, but the summation should be understood as a formal expansion, whose convergence is not guaranteed. Based on the existence of the wave function, we conjecture that the summation over ν will be generally convergent after integrated over t in Eq. (6). Unfortunately, it is difficult to prove this statement, because the integral of Eq. (6) is also involved in $\psi(x_0, t)$, which is unknown as yet. Still, we suggest that $\sin \nu t$ could be an illustrative example: It does not converge when summed over $\nu = 1, 2, \dots$. However, if we first integrate it over t and then carry out the summation, the result can converge to a well-defined value.

Appendix C: Solving Eq. (24) for $c(t)$

Let us rearrange the terms of Eq. (24) as follows:

$$8ik\psi(0,t)c_t(t) + [8ik\psi_t(0,t) - 40k^3\psi(0,t)]c(t) + \pi [\psi_{tt}(0,t) + 10ik^2\psi_t(0,t) - 9k^4\psi(0,t)] \approx 0. \quad (\text{C1})$$

Dividing both sides by $8ik\psi(0,t)$, we get

$$c_t(t) + \left[\frac{\psi_t(0,t)}{\psi(0,t)} + 5ik^2 \right] c(t) \approx \frac{iL}{4\psi(0,t)} [\psi_{tt}(0,t) + 10ik^2\psi_t(0,t) - 9k^4\psi(0,t)], \quad (\text{C2})$$

which is a linear first-order ODE for $c(t)$. Its formal solution takes the form [34]

$$c(t) = e^{-I(t)} \int_0^t dt' Q(t') e^{I(t')} + c(0) e^{-I(t)}, \quad (\text{C3})$$

where

$$\begin{aligned} I(t) &\equiv \int_0^t dt' \left[\frac{\psi_t(0,t')}{\psi(0,t')} + 5ik^2 \right] \\ &= \int_0^t dt' \left\{ \frac{d}{dt'} [\ln \psi(0,t')] + 5ik^2 \right\} \\ &= \ln \psi(0,t) - \ln \psi(0,0) + 5ik^2 t, \end{aligned} \quad (\text{C4})$$

and $Q(t) \equiv \frac{iL}{4\psi(0,t)} [\psi_{tt}(0,t) + 10ik^2\psi_t(0,t) - 9k^4\psi(0,t)]$. If we plug Eq. (C4) into Eq. (C3), the first term on the RHS of Eq. (C3) is evaluated as

$$e^{-I(t)} \int_0^t dt' Q(t') e^{I(t')} = \frac{iL e^{-5ik^2 t}}{4\psi(0,t)} \int_0^t dt' e^{5ik^2 t'} \left(\frac{\partial}{\partial t'} + ik^2 \right) \left(\frac{\partial}{\partial t'} + 9ik^2 \right) \psi(0,t'), \quad (\text{C5})$$

and the second term gives

$$c(0) e^{-I(t)} = \frac{c(0)\psi(0,0)}{\psi(0,t)} e^{-5ik^2 t}. \quad (\text{C6})$$

- [1] A. P. Alivisatos, *Science* **271**, 933 (1996).
- [2] R. H. Swendsen, *An introduction to Statistical Mechanics and Thermodynamics* (Oxford University Press, Oxford, 2012).
- [3] C. Kittel, *Introduction to Solid State Physics* (John Wiley & Sons, Hoboken, NJ, 2005).
- [4] L. Szilard, *Z. Phys.* **53**, 840 (1929).

- [5] W. Zurek, in *Frontiers of Nonequilibrium Statistical Physics*, NATO ASI Series, Vol. 135, edited by G. T. Moore and M. O. Scully (Plenum, New York, 1986) pp. 151–161.
- [6] S. W. Kim, T. Sagawa, S. De Liberato, and M. Ueda, *Phys. Rev. Lett.* **106**, 070401 (2011).
- [7] T. Sagawa and M. Ueda, *Phys. Rev. Lett.* **100**, 080403 (2008).
- [8] K. Jacobs, *Phys. Rev. A* **80**, 012322 (2009).
- [9] S. Toyabe, T. Sagawa, M. Ueda, E. Muneyuki, and M. Sano, *Nat. Phys.* **6**, 988 (2010).
- [10] T. Sagawa and M. Ueda, *Phys. Rev. Lett.* **104**, 090602 (2010); **109**, 180602 (2012); *Phys. Rev. E* **85**, 021104 (2012); in *Nonequilibrium Statistical Physics of Small Systems: Fluctuation Relations and Beyond*, edited by R. Klages, W. Just, and C. Jarzynski (Wiley, Weinheim, 2013) pp. 181–211.
- [11] K. Jacobs, *Phys. Rev. E* **86**, 040106(R) (2012).
- [12] J. M. Horowitz, T. Sagawa, and J. M. R. Parrondo, *Phys. Rev. Lett.* **111**, 010602 (2013).
- [13] J. Um, H. Hinrichsen, C. Kwon, and H. Park, *New J. Phys.* **17**, 085001 (2015).
- [14] The performance of the engine was considered in M. Park, S. D. Yi, and S. K. Baek, *J. Korean Phys. Soc.* **66**, 739 (2015) for the case of a penetrable barrier.
- [15] J. M. Jauch and J. G. Baron, *Helv. Phys. Acta* **45**, 220 (1972).
- [16] A. Messiah, *Quantum mechanics* (North-Holland Pub. Co., Amsterdam, 1961).
- [17] C. M. Bender, D. C. Brody, and B. K. Meister, *Proc. R. Soc. A* **461**, 733 (2005).
- [18] K.-H. Kim and S. W. Kim, *Phys. Rev. E* **84**, 012101 (2011).
- [19] H. R. Lewis Jr., *J. Math. Phys.* **9**, 1976 (1968).
- [20] J.-Y. Ji, J. K. Kim, and S. P. Kim, *Phys. Rev. A* **51**, 4268 (1995).
- [21] W. S. Truscott, *Phys. Rev. Lett.* **70**, 1900 (1993).
- [22] M. Feng, *Phys. Rev. A* **64**, 034101 (2001).
- [23] T. J. Park, *Bull. Korean Chem. Soc.* **23**, 355 (2002).
- [24] L. Pezzé, A. Smerzi, G. P. Berman, A. R. Bishop, and L. A. Collins, *New J. Phys.* **7**, 85 (2005).
- [25] U. Hohenester, P. K. Rekdal, A. Borzì, and J. Schmiedmayer, *Phys. Rev. A* **75**, 023602 (2007); J. Grond, J. Schmiedmayer, and U. Hohenester, **79**, 021603(R) (2009); J. Grond, G. von Winckel, J. Schmiedmayer, and U. Hohenester, **80**, 053625 (2009).
- [26] S. Masuda and K. Nakamura, *Phys. Rev. A* **78**, 062108 (2008); *Proc. R. Soc. A* **466**, 1135 (2009).

- [27] E. Torrontegui, S. Martínez-Garaot, M. Modugno, X. Chen, and J. G. Muga, *Phys. Rev. A* **87**, 033630 (2013).
- [28] Y. Shin, M. Saba, T. A. Pasquini, W. Ketterle, D. E. Pritchard, and A. E. Leanhardt, *Phys. Rev. Lett.* **92**, 050405 (2004).
- [29] M. Albiez, R. Gati, J. Fölling, S. Hunsmann, M. Cristiani, and M. K. Oberthaler, *Phys. Rev. Lett.* **95**, 010402 (2005).
- [30] C. Van den Broeck, *Phys. Rev. Lett.* **95**, 190602 (2005).
- [31] M. Esposito, K. Lindenberg, and C. Van den Broeck, *Phys. Rev. Lett.* **102**, 130602 (2009).
- [32] M. Esposito, R. Kawai, K. Lindenberg, and C. Van den Broeck, *Phys. Rev. Lett.* **105**, 150603 (2010).
- [33] J. Campbell, *J. Phys. A* **42**, 365212 (2009).
- [34] M. L. Boas, *Mathematical Methods in the Physical Sciences*, 3rd ed. (Wiley, Hoboken, NJ, 2006).
- [35] M. E. J. Newman, *Computational Physics* (CreateSpace Independent, United States, 2013).
- [36] J. Gea-Banacloche, *Am. J. Phys.* **70**, 307 (2002); M. Lakner and J. Peternej, **71**, 519 (2003); S. J. van Enk, **77**, 140 (2009).
- [37] K.-H. Kim and S. W. Kim, *J. Korean Phys. Soc.* **61**, 1187 (2012).
- [38] T. P. Meyrath, F. Schreck, J. L. Hanssen, C.-S. Chuu, and M. G. Raizen, *Phys. Rev. A* **71**, 041604(R) (2005).
- [39] K. Henderson, H. Kelkar, T. C. Li, B. Gutiérrez-Medina, and M. G. Raizen, *EPL* **75**, 392 (2006).
- [40] C. Zhang, K. Nho, and D. P. Landau, *Phys. Rev. A* **77**, 025601 (2008).
- [41] N. D. Antunes, F. C. Lombardo, D. Monteoliva, and P. I. Villar, *Phys. Rev. E* **73**, 066105 (2006).